JOURNAL OF MATERIALS SCIENCE **39** (2004) 1891 – 1893

Shear strength of ceramics

XIAOTONG WANG, N. P. PADTURE*
Department of Metallurgy and Materials Engineering, Institute of Materials Science, University of Connecticut, Storrs, CT 06269-3136, USA
E-mail: nitin.padture@uconn.edu

Nanoindentation experiments [1, 2], Bragg-Nye bubble-raft simulation experiments [3], and atomistic/finite-element modeling [4] have revealed that incipient plasticity in ductile metals occurs at shear stress values approaching the theoretical shear strength. This incipient plasticity, characterized by a sudden burst of displacement in the nanoindentation load-depth (*P*-*h*) response at sub-milliNewton loads (0.01 to 0.03 mN for single-crystal Al) [2], represents homogeneous nucleation of defects such as dislocations. In order to investigate if incipient plasticity can be detected quantitatively in brittle ceramics using displacement bursts in nanoindentation *P*-*h* responses, we have performed low-load nanoindentation experiments on two single-crystals: Y_2O_3 and $SrTiO_3$, cubic ceramics whose shear moduli differ by about a factor of two. We have found that displacement bursts in the nanoindentation *P*-*h* responses occur at average indentation loads of 0.15 and 0.65 mN in Y_2O_3 and $SrTiO_3$, respectively, and that these loads are consistent with the calculated theoretical shear strengths of the two ceramics.

Single-crystal $SrTiO_3$ (100) was obtained commercially (Material-Technologie & Kristalle Gmbh, Germany), whereas a polished large-grain size (100 μm) Y_2O_3 polycrystalline specimen was obtained from Dr. W. H. Rhodes. While the (100) surface of the $SrTiO_3$ single-crystal was indented, the orientation of the indented grain in the Y_2O_3 was unknown. Approximately 50 nanoindentation experiments were performed on each material at different surface locations, using Nanoindenter XP (MTS/Nanoinstrument, Oak Ridge, TN), in Dynamic Contact Module^{TM} (DCM) mode, equipped with a diamond Berkovich pyramid. The peak load ranged from 0.1 to 1.0 mN, while the total loading time required to reach the peak load was maintained constant at 30 s.

Fig. 1A and B show representative *P*-*h* curves for the nanoindentation of Y_2O_3 and $SrTiO_3$, respectively. Note the displacement bursts at indentation loads (P^*) of 0.145 and 0.625 mN in Y_2O_3 and $SrTiO_3$, respectively. The indentation loads at *P*-*h* discontinuities for Y_2O_3 ranged from 0.1 to 0.2 mN, with an average of $P^* = 0.15$ mN. In the case of $SrTiO_3$, P^* ranged between 0.5 and 0.8 mN, with an average of $P^* = 0.65$ mN. A hard "dummy" specimen (SiC) was nanoindented several times (at different locations) under the same conditions, where no displacement bursts were observed. This confirmed that the observed displacements bursts in Y_2O_3 and $SrTiO_3$ are not an artifact of the instrument, and that those bursts arise from material response alone.

The maximum shear stress under the Berkovich indenter at indentation load P^*, where the *P*-*h* discontinuity occurs, can be determined using the following relation [2, 5]:

$$\tau_{\text{Max}} = 0.31\left(\frac{6P * E^{*^2}}{\pi^3 R^2}\right)^{0.33}, \tag{1}$$

where *R* is the radius of the tip of the indenter, and E^* is defined in terms of the Young's moduli and the Poisson's ratios of the diamond indenter (E_i, ν_i) and the specimen (E_s, ν_s) as follows [2, 5]:

$$E* = \left(\frac{1-\nu_s^2}{E_s} + \frac{1-\nu_i^2}{E_i}\right)^{-1}. \tag{2}$$

Although the Berkovich pyramid is a "sharp" indenter, it has a finite radius, which is assumed to be $R \sim 50$ nm for a new indenter [2]. Using the values for elastic properties of diamond, Y_2O_3, and $SrTiO_3$ (Table I), the maximum shear stress values τ_{Max} at *P*-*h* discontinuities for Y_2O_3 and $SrTiO_3$ are calculated to be 16.1 and 34.1 GPa, respectively (Table I). A rough estimate for the theoretical shear strength of crystals is given by [6]:

$$\tau_{\text{Th}} = G/2\pi, \tag{3}$$

where *G* is the shear modulus of the specimen, which is given by [6]:

$$G = \frac{E_s}{2(1+\nu_s)}. \tag{4}$$

Using Equations 3 and 4, the theoretical shear strengths for Y_2O_3 and $SrTiO_3$ are calculated, and they are also given in Table I, along with $\tau_{\text{Max}}/\tau_{\text{Th}}$ ratios. Although the estimate of the theoretical shear strength is only an approximation (Equations 3) [6], these ratios are not significantly different compared with unity (1.5 and 1.7), indicating that τ_{Max} represents the theoretical shear strength of the ceramic in question. This notion is further reinforced by the fact that the $\tau_{\text{Max}}/\tau_{\text{Th}}$ ratios for the two ceramics are not very different. The local breakdown of the material could be manifest as fracture or

*Author to whom all correspondence should be addressed.

0022–2461

TABLE I Relevant mechanical properties of ceramics, and calculated values of τ_{Max} (Equation 1) and τ_{Th} (Equation 3)

Ceramic	P^* (GPa)	E (GPa)	ν	G (GPa)	τ_{Max} (GPa)	τ_{Th} (GPa)	τ_{Max}/τ_{Th}
Y_2O_3	0.15	172 [12]	0.31 [12]	66 [12]	16.1	10.5	1.5
$SrTiO_3$	0.65	300 [13]	0.20 [13]	125 [13]	34.1	19.9	1.7
Diamond	–	1000 [2]	0.07 [2]	–	–	–	–
MgO	1.0 [7]	290 [11]	0.19 [11]	130 [11]	38.5	19.4	2.0
Al_2O_3	15 [9]	400 [10]	0.22 [10]	164	110.8	26.1	4.2

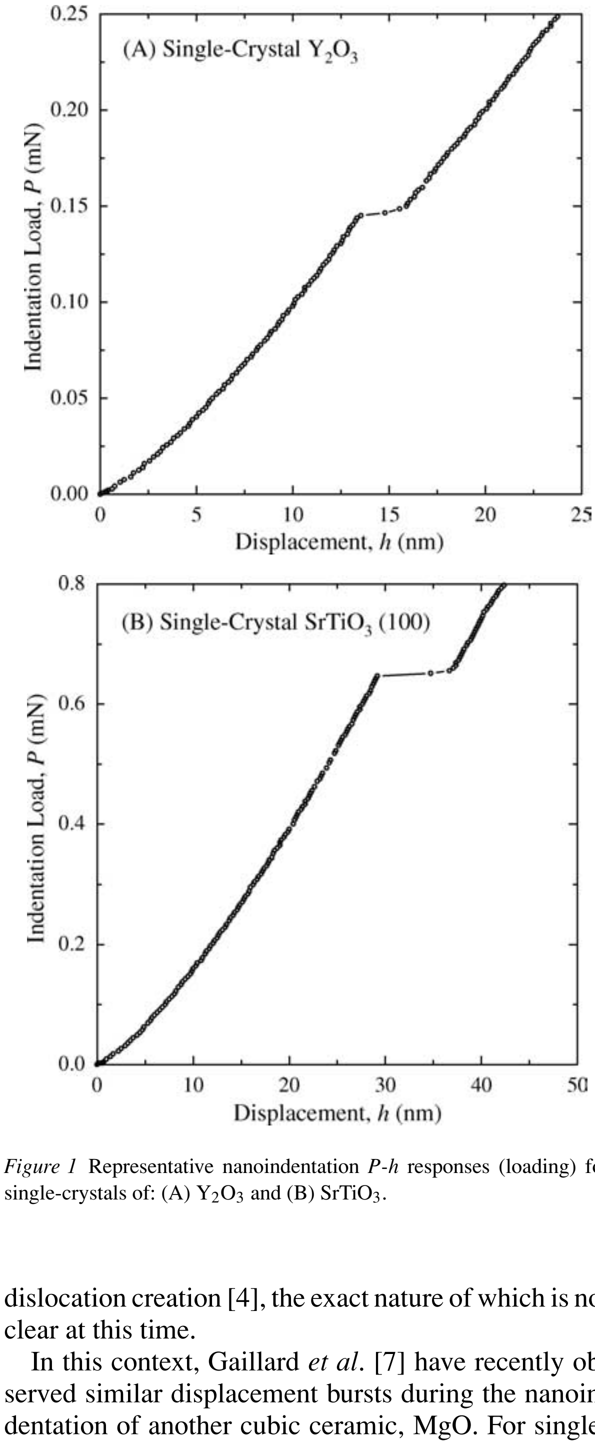

Figure 1 Representative nanoindentation P-h responses (loading) for single-crystals of: (A) Y_2O_3 and (B) $SrTiO_3$.

dislocation creation [4], the exact nature of which is not clear at this time.

In this context, Gaillard *et al.* [7] have recently observed similar displacement bursts during the nanoindentation of another cubic ceramic, MgO. For single-crystal MgO (001) specimens, the indentation load at which this burst occurs (P^*) is 1.0 mN. However, the displacement burst in terms of indentation depth (h) in MgO (25 nm) [7] was found to be significantly greater than that observed for Y_2O_3 (3 nm) and $SrTiO_3$ (7 nm). Using Equations 1 to 4 and elastic-property values (Table I) in the case of MgO, the τ_{Max}/τ_{Th} ratio was found to be 2.0, which, once again, is consistent with τ_{Max} identifying with the theoretical shear strength of MgO.

Gaillard *et al.* [7] have also performed careful etching experiments on nanoindented MgO, which is a way to reveal dislocations that intersect the free surface [8], and they have characterized the resulting etch-pits using the atomic force microscope (AFM). For nanoindentation loads greater than P^*, they have found well-defined patterns of etch-pits around the nanoindentation site [7]. For $P < P^*$, the etching results were inconclusive [7]. These results suggest that the displacement bursts in nanoindentation of cubic ceramics are associated with the nucleation of dislocations.

Page *et al.* [9] were the first to report nanoindentation displacement bursts in ceramics. However, they found the burst to occur at much higher loads (P^* for single-crystal $Al_2O_3 \sim 15$ mN). Using Equations 1 to 4 and elastic-property values (Table I) in the case of rhomohedral Al_2O_3, the τ_{Max}/τ_{Th} ratio is found to be 4.2, which is higher than that for cubic ceramics. This could be possibly due to the reduced crystal symmetry in Al_2O_3. Page *et al.* [9] have also attributed these bursts to the formation of incipient cracks in Al_2O_3.

In the case of metals, multiple displacement bursts have been observed, which occur at successively higher nanoindentaion loads P, and over larger h ranges [2]. It has been shown that this is due to the motion of the already formed dislocations, which requires orders of magnitude lower shear stresses (identifies with the Peierls stress) relative to theoretical shear strengths. In the nanoindentation of brittle ceramics, such multiple displacement bursts are not common, possibly due to the very high values of the Peierls stress relative to ductile metals [10, 11].

In summary, the displacement bursts we have observed during the nanoindentation of ceramics arise as a result of material response, and are not an instrument artifact. In the case of cubic ceramics, the maximum shear stress (τ_{Max}) associated with the nanoindentation load at which these bursts occur identifies with the respective theoretical shear strength (τ_{Th}) of the ceramic in question. It appears that homogenous nucleation of dislocations is responsible for the displacement burst, however, further work is needed to elucidate this issue.

Acknowledgments
The authors thank Prof. S. Suresh (MIT) and Dr. D. T. Smith (NIST) for fruitful discussions, and Dr. R. H. Rhodes for providing the Y_2O_3 specimen. Partial funding for this work was provided by the Office of Naval Research through a subcontract from MIT (prime grant DURINT N00014-01-1-0808).

References

1. W. W. GERBERICH, J. C. NELSON, E. T. LILLEODDEN, P. ANDERSON and J. T. WYROBEK, *Acta Mater.* **166** (1996) 299.
2. A. GOULDSTONE, H. J. KOH, K. Y. ZENG, A. E. GIANNAKOPOULOS and S. SURESH, *ibid.* **48** (2000) 2277.
3. A. GOULDSTONE, K. J. VANVLIET and S. SURESH, *Nature* **411** (2001) 656.
4. J. LI, K. J. VANVLIET, T. ZHU, S. YIP and S. SURESH, *ibid.* **418** (2002) 307.
5. K. L. JOHNSON, "Contact Mechanics" (Cambridge University Press, Cambridge, UK, 1985).
6. T. H. COURTNEY, "Mechanical Behavior of Materials" (McGraw Hill, New York, 2000).
7. T. GAILLARD, C. TROMAS and J. WOIRGARD, *Acta Mater*. **51** (2003) 1059.
8. J. J. GILMAN, W. G. JOHNSTON and G. W. SEARS, *J. Appl. Phys*. **29** (1958) 747.
9. T. F. PAGE, W. C. OLIVER and C. J. MCHARGUE, *J. Mater. Res*. **7** (1992) 450.
10. B. R. LAWN, "Fracture of Brittle Solids," 2nd ed. (Cambridge University Press, Cambridge, UK, 1993).
11. J. B. WACHTMAN, "Mechanical Properties of Ceramics" (John Wiley & Sons, New York, NY, 1996).
12. J. W. PALKO, W. M. KRIVEN, S. V. SINOGEIKIN, J. D. BASS and A. SAYIR, *J. Appl. Phys*. **89** (2001) 7791.
13. K. H. HELLWEGE and A. M. HELLWEGE, "Landolt-Bornstein New Series: Group III," Vol. 16, Oxides (Springer-Verlag, New York, NY, 1981) p. 64.

Received 13 August
and accepted 16 September 2003